This is the accepted manuscript made available via CHORUS. The article has been published as:

Black hole spectroscopy in the next decade

Miriam Cabero, Julian Westerweck, Collin D. Capano, Sumit Kumar, Alex B. Nielsen, and Badri Krishnan

Phys. Rev. D **101**, 064044 — Published 20 March 2020

DOI: 10.1103/PhysRevD.101.064044

The next decade of black hole spectroscopy

Miriam Cabero,[1,*] Julian Westerweck,[2,3] Collin D. Capano,[2,3]
Sumit Kumar,[2,3] Alex B. Nielsen,[2,3,4] and Badri Krishnan[2,3]

[1] *Department of Physics, Princeton University, Princeton, NJ 08544, USA*
[2] *Max Planck Institute for Gravitational Physics (Albert Einstein Institute), Callinstrasse 38, D-30167 Hannover, Germany*
[3] *Leibniz Universität Hannover, Welfengarten 1-A, D-30167 Hannover, Germany*
[4] *Department of Mathematics and Physics, University of Stavanger, 4036 Stavanger, Norway*

Gravitational wave observations of the ringdown of the remnant black hole in a binary black hole coalescence provide a unique opportunity of confronting the black hole no-hair theorem in general relativity with observational data. The most robust tests are possible if multiple ringdown modes can be observed. In this paper, using state-of-the-art Bayesian inference methods and the most up-to-date knowledge of binary black hole population parameters and ringdown mode amplitudes, we evaluate the prospects for black hole spectroscopy with current and future ground based gravitational wave detectors over the next 10 years. For different population models, we estimate the likely number of events for which the subdominant mode can be detected and distinguished from the dominant mode. We show that black hole spectroscopy could significantly test general relativity for events seen by the proposed LIGO Voyager detectors.

I. INTRODUCTION

The remnant black hole (BH) formed after the coalescence of two compact objects emits gravitational radiation while settling down to a Kerr BH. This stage is known as the ringdown. Perturbation theory predicts that, at late enough times, the ringdown consists of a superposition of exponentially damped sinusoids called quasinormal modes (QNM) [1, 2] (see also [3, 4]). The QNMs are characterized by a set of complex frequencies $\Omega_{\ell mn}$ labeled by three integers; ℓ, m are angular quantum numbers while $n = 0, 1, 2\ldots$ is the overtone index. According to the no-hair theorem in standard general relativity (GR), $\Omega_{\ell mn}$ is uniquely defined by the BH mass and spin. The measurement of multiple QNMs in a BH ringdown, known as BH spectroscopy, is crucial for robust observational tests of the no-hair theorem with gravitational waves based only on the ringdown signal [5, 6].

The excitation of different QNMs depends on the nature of the perturbation, i.e. on the properties of the binary progenitor [7–11]. Thus, for aligned spin systems, the amplitude of the different modes are determined by the spins of the initial compact objects and the mass ratio $q = m_1/m_2 \geq 1$, with $m_{1,2}$ the mass of each object. The ringdown signature is dominated by the fundamental $(\ell, m) = (2, 2)$ mode [12]. For non-spinning binaries with equal masses ($q = 1$), odd ℓ modes vanish and the loudest subdominant mode is the $(\ell, m) = (4, 4)$ mode. As the mass ratio increases, the $(\ell, m) = (3, 3)$ mode becomes the loudest subdominant mode, with amplitudes larger than 30% of the dominant amplitude ($A_{330}/A_{220} > 0.3$) [7, 8]. Hence, coalescences of two unequal-mass BHs or neutron-star black-hole binaries (NSBH) are the most promising sources for measurability of subdominant modes in the ringdown. For still higher mass ratios, the relative amplitude of the modes can also tell us about the alignment of the orbit relative to the BH spin during the inspiral phase [9–11].

Two main conditions are necessary to test the no-hair theorem: (i) the detectability of at least two modes, and (ii) the resolvability of the frequencies and/or damping times of each mode. Theoretical estimates of the necessary ringdown signal-to-noise ratio (SNR) for each of these conditions can be found in the literature [6, 13]. These studies have predicted that Advanced LIGO should observe several ringdown events at design sensitivity, but will not be able to detect subdominant modes from the coalescence of stellar-mass BBH for BH spectroscopy [14, 15]. In this paper we revisit the prospects for accurate BH spectroscopy with the next decade of LIGO detectors. In general, asymmetric binaries are more likely to produce higher amplitudes for the subdominant ringdown modes. However, based on the gravitational-wave observations to date, more asymmetric systems are also likely to be much fewer in number [16] (although recent public alerts from the third observing run of Advanced LIGO and Virgo suggest possible detections of NSBH [17, 18]). In addition, the orientation of a source relative to the detectors also has an important effect on the observed amplitudes. Systems where the angular momentum is aligned with the line-of-sight to the source are more luminous, but these orientations are not favorable for observing the subdominant modes. Taking all these effects into account, along with the most up-to-date estimates of the ringdown mode amplitudes [8] and state-of-the-art gravitational wave parameter estimation techniques [19, 20], we show that black hole spectroscopy can provide non-trivial limits on general relativity with the LIGO Voyager detector.

At least 10 binary black-hole (BBH) coalescences have been observed in the first two observing runs of Advanced LIGO and Virgo [21–26]. The loudest BBH event is still the first detection, GW150914 [27], with a ringdown signal-to-noise ratio (SNR) $\rho \simeq 8.5$ [28] at 3 ms after

* mcmuller@princeton.edu

merger. This event has not provided significant evidence for the presence of measurable subdominant modes with $\ell \neq 2$ [29]. However, recent work suggests that the inclusion of higher overtones of the dominant $\ell = 2$ mode allows for the modeling of the ringdown immediately after the merger, hence obtaining higher SNR in ringdown signatures [30]. The analysis of the GW150914 ringdown using the fundamental mode and its first overtone provides the first constraints to date of deviations of the no-hair theorem using two QNMs [31]. Here we use the Bayesian inference and model selection frameworks [32] on simulated BBH populations to establish the measurability and accurate resolvability of two ringdown QNMs over the next decade, providing rate estimates for constraining the no-hair theorem to within $\pm 20\%$ at the 90% credible level. We restrict ourselves to the resolvability of subdominant QNMs ($\ell \neq 2$) for two reasons: (1) the excitation amplitudes of overtones on the general parameter space of the binary's properties are not yet well-understood and we lack predictions to model ringdown signatures that include overtones for a large population of BBH mergers, and (2) the frequencies of the overtones are very similar to each other, hence accurate resolvability of an overtone is more challenging than of a subdominant mode.

This manuscript is organized as follows. Section II introduces the Bayesian inference and model selection frameworks, as well as the ringdown model used. Section III describes the details on the BBH population considered. In Section IV we report the rates on measurable subdominant modes and prospects for resolvability of the necessary parameters to perform tests of the no-hair theorem. Finally, we conclude our findings in Sec. V.

II. BAYESIAN FRAMEWORK

We use Bayesian methods to infer the properties of the remnant BH from our data, $d(t)$, and to determine the presence of a measurable subdominant mode in the ringdown signature. Given a model hypothesis of the ringdown signal, H, parametrized by the source properties, $\vec{\vartheta}$, Bayes' theorem defines the posterior probability distribution:

$$p(\vec{\vartheta}|d,H) = p(\vec{\vartheta}|H)\frac{p(d|\vec{\vartheta},H)}{p(d|H)}\,, \tag{1}$$

where $p(\vec{\vartheta}|H)$ is the prior knowledge based on astrophysical populations or theoretical models, the likelihood $p(d|\vec{\vartheta},H)$ is the conditional probability of observing the data $d(t)$ given the model H with parameters $\vec{\vartheta}$, and the evidence $p(d|H)$ is a normalization constant that only depends on the data and the chosen model. Calculating the evidence requires marginalization over the entire parameter space, which can become computationally challenging. While this computation can be avoided for Bayesian parameter estimation, model selection between two competing models requires accurate estimates of the evidence.

In Bayesian model selection, the Bayes factor weighs the evidence provided by the data in support of one model versus another [32, 33]:

$$\mathcal{B}_{AB} = \frac{p(d|H_A)}{p(d|H_B)}\,. \tag{2}$$

In this manuscript we follow the nomenclature of [32]: a Bayes factor $\mathcal{B}_{AB} > 3.2$ indicates "substantial" support for H_A over H_B, $\mathcal{B}_{AB} > 10$ indicates "strong" support, while $\mathcal{B}_{AB} > 100$ is "decisive".

A. The likelihood function

For a GW detector network with uncorrelated stationary Gaussian noise, the likelihood is given by

$$p(d|\vec{\vartheta},H) \propto \exp\left[-\frac{1}{2}\sum_{a=1}^{N}\langle d_a - h_a(\vec{\vartheta}), d_a - h_a(\vec{\vartheta})\rangle\right]\,, \tag{3}$$

where N is the number of detectors, d_a is the data for each detector, and $h_a(\vec{\vartheta})$ is the waveform model evaluated for a set of parameters $\vec{\vartheta}$ as observed by detector a. The noise-weighted inner product is defined as

$$\langle x, y\rangle = 4\Re\int_0^\infty \frac{\tilde{x}^*(f)\tilde{y}(f)}{S_n(f)}\mathrm{d}f\,, \tag{4}$$

with $S_n(f)$ being the one-sided power spectral density (PSD) of the detector's noise, $\tilde{x}(f)$ the Fourier transform of $x(t)$, and * indicating the complex conjugate.

In this paper we use the `PyCBC Inference` [19, 20] toolkit to compute the likelihood function and estimate posterior probability distributions. Accurate marginalization for evidence estimation is achieved using the nested sampling algorithm `cpnest` [34].

B. The ringdown model

The strain $h(t)$ produced by a gravitational wave at the detector is given by

$$h(t) = F_+(\alpha,\delta,\Psi)h_+(t) + F_\times(\alpha,\delta,\Psi)h_\times(t)\,, \tag{5}$$

where $F_{+,\times}$ are the antenna pattern functions determined by the relative orientation between the detector frame and the wave frame [35], i.e. the sky location of the source (right ascension α and declination δ in a geocentric coordinate system) and the polarization angle Ψ that defines the relative orientation of the wave frame with the geocentric coordinate system. For short transient signals, these orientation angles (and hence $F_{+,\times}$) are assumed to be time independent. For future generation of observatories with improved low frequency sensitivity, it might

become necessary to account for the time dependence of $F_{+,\times}$. However, the ringdown itself will be short enough that for our purposes we do not need to consider this effect here.

The ringdown signal of a Kerr BH consists of a sum of exponentially damped sinusoids:

$$h_+ + ih_\times = \frac{M}{D_L}\sum_{\ell,m,n} {}_{-2}S_{\ell m}(\iota,\varphi) A_{\ell mn} e^{i(\Omega_{\ell mn}t+\phi_{\ell mn})}\,, \tag{6}$$

where M is the mass of the BH in the detector frame and D_L is the luminosity distance to the source. The functions ${}_{-2}S_{\ell m}(\iota,\varphi)$ are the spin-weighted spheroidal harmonics, which depend on the inclination angle ι between the BH spin and the line-of-sight from the observer to the source, and the azimuth angle φ between the BH and the observer. The complex QNM frequencies $\Omega_{\ell mn}$, determined from the Teukolsky equation [36, 37], define the frequency and damping time of the damped sinusoid, $\Omega_{\ell mn} = \omega_{\ell mn} + i/\tau_{\ell mn}$. The amplitudes $A_{\ell mn}$ and $\phi_{\ell mn}$ depend on the initial perturbation and take different values for different (ℓ, m, n) modes. Henceforth, we restrict ourselves to the $n = 0$ overtone and drop the overtone index n for simplicity.

Assuming that the ringdown begins at $t = 0$, the two gravitational-wave polarizations are given by

$$\begin{aligned} h_+(t) &= \frac{M}{D_L}\sum_{\ell,m} {}_{-2}Y^{+}_{\ell m}(\iota) A_{\ell m} e^{-t/\tau_{\ell m}} \cos(\omega_{\ell m}t+\phi_{\ell m})\,,\\ h_\times(t) &= \frac{M}{D_L}\sum_{\ell,m} {}_{-2}Y^{\times}_{\ell m}(\iota) A_{\ell m} e^{-t/\tau_{\ell m}} \sin(\omega_{\ell m}t+\phi_{\ell m})\,, \end{aligned} \tag{7}$$

where we have approximated the spheroidal harmonics ${}_{-2}S_{\ell m}$ by spin-weighted spherical harmonics ${}_{-2}Y_{\ell m}$ [13, 38]:

$$\begin{aligned} {}_{-2}Y^{+}_{\ell m}(\iota) &= {}_{-2}Y_{\ell m}(\iota,0) + (-1)^{\ell}\,{}_{-2}Y_{\ell\text{-}m}(\iota,0)\,,\\ {}_{-2}Y^{\times}_{\ell m}(\iota) &= {}_{-2}Y_{\ell m}(\iota,0) - (-1)^{\ell}\,{}_{-2}Y_{\ell\text{-}m}(\iota,0)\,. \end{aligned} \tag{8}$$

The ringdown analysis in this paper follows the methods developed in [39, 40]. We use two different waveform models, (i) a *Kerr model* where we assume the remnant object to be a Kerr BH, hence the ringdown QNM frequencies $\Omega_{\ell mn}$ are uniquely determined by the mass M and the spin χ of the BH, and (ii) an *agnostic model* where we assume the nature of the remnant object to be unknown, hence the ringdown is parameterized by each individual QNM frequency $\Omega_{\ell mn}$ and we drop the factor M/D_L in Eq. (7). The Kerr model (i) is our starting point for determining the measurability of a subdominant mode. Resolvability of the subdominant mode for testing the no-hair theorem is determined using the agnostic model (ii).

III. POPULATIONS

We construct populations of candidate BBH ringdown signals based on the observational population model B of [16] (we ignore NSBH mergers here because population models including NSBH are largely uncertain). The component-mass and mass-ratio distributions follow power laws with exponents $-\alpha$ and β_q, respectively (see Eq. (2) in [16]). For the component-mass distribution, we use the measured median value $\alpha = 1.6$, with masses in the range $[5.4, 57)M_\odot$ (we use the lowest m_{min} and the largest m_{max} values, to account for uncertainties in the mass bounds of BHs). For the mass-ratio distribution we use two different exponent values: the measured median value $\beta_q = 6.7$, and a uniform distribution $\beta_q = 0$ (which is used in model A of [16]). Mass ratios are restricted to be within the range $[1, 8)$. We assume the individual BHs to be non-spinning prior to the merger, which is consistent with the population of BBHs observed by LIGO/Virgo thus far. Sources are distributed uniformly in co-moving volume; we choose a maximum luminosity distance, $D_L^{(\max)}$, dependent on the considered detector network. The inclination angle ι is distributed uniformly in $\cos\iota \in [-1, 1)$, and the polarization angle ψ uniformly $\in [0, 2\pi)$.

The mass and spin of the remnant Kerr BH determine the ringdown frequencies $\Omega_{\ell m}$ [41]. We obtain an estimate of the remnant's source frame mass $M^{(\mathrm{src})}$ and dimensionless spin χ using the fitting formulae to numerical relativity [42, 43] implemented in the `LALSuite` software package [44]. The detector frame mass M is given by $M = (1+z)M^{(\mathrm{src})}$, where z is the redshift calculated from the luminosity distance, D_L, assuming a standard ΛCDM cosmology [45]. The excitation amplitudes $A_{\ell m}$, which depend on the mass ratio q of the binary, are determined using the fitting formulae in [8] at $t = 10M$ after the merger. The phases $\phi_{\ell m}$ of the modes are distributed uniformly in $\phi_{\ell m} \in [0, 2\pi)$, in contrast to previous work in the literature where both phases were fixed for simplicity [13, 46, 47].

The BBH parameters for each candidate are drawn randomly from their respective distributions to generate two-mode ringdown signals with the dominant $(\ell, m) = (2, 2)$ mode and either the $(\ell, m) = (3, 3)$ or the $(\ell, m) = (4, 4)$ subdominant mode. We consider a three-detector LIGO network consisting of the observatories in Hanford (H1), Livingston (L1) and India (I1). We use three different sensitivities for these detectors [48]: Advanced LIGO design sensitivity (Adv. LIGO), A+ and Voyager. We do not consider here the complete third generation detectors, which include the Einstein Telescope [49–51] and Cosmic Explorer [52], or the space based LISA mission [53], since this would take us beyond the 10-year timeframe.

For each candidate, we calculate the optimal SNR of the subdominant mode in each detector, $\rho_{\mathrm{det}} = \sqrt{\langle h, h\rangle}$, where h is the ringdown signal of the subdominant mode projected into the detector (see Eqs. (5) and (7)). To

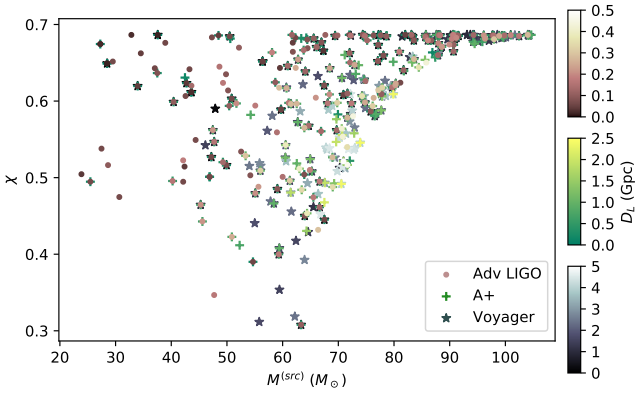

FIG. 1. Source frame mass, $M^{(\mathrm{src})}$, and spin, χ, of the BHs with optimal SNR $\rho_c \geq 2.5$ in the subdominant mode (either the $(3,3)$ or the $(4,4)$ mode), obtained using the observational population models of [16]. The colors represent the luminosity distance of the source, where the maximum allowed distance was $D_L^{(\mathrm{max})} = \{1,3,5\}$ Gpc for Adv. LIGO, A+ and Voyager, respectively.

avoid a large number of sources with no measurable subdominant mode, we reject candidates with combined optimal SNR $\rho_c = \sqrt{\sum_{\mathrm{det}} \rho^2_{\mathrm{det}}} < 2.5$ in the subdominant mode. For the same reason, the maximum D_L considered is limited to different values for different sensitivities, namely $D_L^{(\mathrm{max})} = \{1,3,5\}$ Gpc for Adv. LIGO, A+ and Voyager, respectively. The number of draws required to find a sample population of 100 signals with $\rho_c \geq 2.5$ in the subdominant mode yields the fraction of interesting candidates out of all BBH signals. Figure 1 shows the resulting populations for each detector network considered.

IV. ANALYSIS AND RESULTS

A. Rates of measurable subdominant modes

We add the population of accepted candidate ringdown signals (shown in Fig. 1) into different Gaussian noise realizations colored with the PSD of the desired detector. To determine the measurability of the subdominant mode, we use the Kerr BH ringdown model and perform two separate Bayesian parameter estimation analyses using: (H_A) templates with the fundamental $(2,2)$ mode plus the corresponding (ℓ, m) subdominant mode, and (H_B) templates with only the fundamental $(2,2)$ mode. The Bayes factor $\mathcal{B}_{AB}$ is then calculated as the ratio of the evidences for model H_A versus model H_B. Those sources with $\mathcal{B}_{AB} > 3.2$ are further analyzed in the next section to determine the resolvability of the subdominant mode.

The parameters $(M,\ \chi,\ A_{\ell m},\ \phi_{\ell m},\ \iota,\ \psi)$ are estimated from the data, which represents a set of 8 parameters in the two-mode ringdown H_A, and 6 parameters in the single-mode ringdown H_B. The priors used in the parameter estimation analysis are uniform in all parameters: BH mass $M \in [10, 200) M_\odot$, BH spin $\chi \in [-0.99, 0.99)$, log-amplitude of the fundamental mode $\log_{10}(A_{22}) \in [-4, 4)$, relative subdominant mode amplitude $\hat{A}_{\ell m} = A_{\ell m}/A_{220} \in [0, 0.5)$, ringdown phases $\phi_{\ell m} \in [0, 2\pi)$, polarization angle $\psi \in [0, 2\pi)$, and inclination angle $\cos(\iota) \in [-1, 1)$. We fix the start time of the ringdown, the (ℓ, m) of the subdominant mode, the sky location and the distance to the source to the injected values. While the start time of the ringdown is not uniquely defined in the literature, we do not explore the issue in this paper and assume that this can be determined by other means [29, 40, 54]. Further, we can safely assume that we have some knowledge from the inspiral part of the signal regarding the mass ratio of the binary to determine which is the loudest subdominant mode to look for. Since we are using a network of three detectors, the sky location should be relatively well known from the analysis of the full gravitational-wave signal. Finally, while the distance might not be accurately measured, fixing this parameter to a wrong value will only affect the measurement of the fundamental amplitude A_{22} and not affect our conclusions.

We calculate the rate of ringdown events with detectable subdominant mode in each detector network based on the BBH merger rate density given in [16] ($R = 53.2^{+58.5}_{-28.8}$ Gpc^{-3} yr^{-1}) and the co-moving volume up to $D_L^{(\mathrm{max})}$ for each detector network. Table I lists the rate of events per year with substantial ($\mathcal{B}_{AB} > 3.2$), strong ($\mathcal{B}_{AB} > 10$), and decisive ($\mathcal{B}_{AB} > 100$) support for the presence of a subdominant mode. These rates are the combination of both the $(3,3)$ and the $(4,4)$ modes. While we have made the simplifying assumption that only one subdominant mode will be measurable, some of the considered BBH systems might have two subdominant modes with SNR $\rho_c \geq 2.5$. However, studying the performance of a three-mode ringdown Bayesian analysis is beyond the scope of this paper.

B. Resolvable subdominant modes for testing GR

In the presence of two measurable ringdown modes, resolvability of the $\Omega_{\ell m}$ frequencies allows for BH spectroscopy tests. However, QNMs of rotating BHs in modified theories of gravity have not been calculated [55], and Kerr-like exotic compact objects can have the same or similar QNM spectrum as Kerr BHs [56]. While it might be challenging to disprove all BH alternatives, accurate measurements of the QNM spectrum will be crucial to constrain deviations from GR (see however [57] for possible ways of parameterizing frequencies and damping times accounting for deviations from GR). It has been shown for non-rotating alternative BH models that GR deviations are more significant in the QNM frequencies than in the damping times [58]. Hence, we focus here on constraining deviations from the subdominant mode's

	$\beta_q = 0$			$\beta_q = 6.7$		
	$\mathcal{B}_{AB} > 3.2$	$\mathcal{B}_{AB} > 10$	$\mathcal{B}_{AB} > 100$	$\mathcal{B}_{AB} > 3.2$	$\mathcal{B}_{AB} > 10$	$\mathcal{B}_{AB} > 100$
Adv. LIGO	$0.036^{+0.039}_{-0.019}$	$0.028^{+0.031}_{-0.015}$	$0.011^{+0.012}_{-0.006}$	$0.008^{+0.009}_{-0.004}$	$0.006^{+0.007}_{-0.003}$	$0.003^{+0.003}_{-0.001}$
A+	$0.46^{+0.51}_{-0.25}$	$0.28^{+0.31}_{-0.15}$	$0.14^{+0.15}_{-0.07}$	$0.08^{+0.09}_{-0.04}$	$0.06^{+0.06}_{-0.03}$	$0.03^{+0.03}_{-0.02}$
Voyager	$2.63^{+2.89}_{-1.42}$	$1.83^{+2.01}_{-0.99}$	$0.89^{+0.97}_{-0.48}$	$0.30^{+0.33}_{-0.16}$	$0.21^{+0.24}_{-0.12}$	$0.11^{+0.12}_{-0.06}$

TABLE I. Rates of BBH ringdown signals per year (yr^{-1}) with a detectable subdominant $(3,3)$ or $(4,4)$ mode for a population with uniform mass-ratio distribution ($\beta_q = 0$) and for a population with $\beta_q = 6.7$. The Bayes factors in each column indicate substantial support ($\mathcal{B}_{AB} > 3.2$), strong support ($\mathcal{B}_{AB} > 10$), and decisive support ($\mathcal{B}_{AB} > 100$) for the presence of a second mode.

frequency.

We consider those ringdown events with $\mathcal{B}_{AB} > 3.2$ in the previous section and perform the same parameter estimation analysis, now using the agnostic model defined in Sec. II B to estimate the ringdown $\Omega_{\ell m}$ frequencies of the two QNMs. Hence, 10 parameters ($\omega_{\ell m}$, $\tau_{\ell m}$, $A_{\ell m}$, $\phi_{\ell m}$, ι, ψ) are now estimated from the data. The priors are uniform in the frequencies $f_{\ell m} = \omega_{\ell m}/2\pi \in [50, 1024)$ Hz and damping times $\tau_{\ell mn} \in [0.45, 30)$ ms, excluding parameters that yield masses and spins outside of the ranges used in the previous section with the Kerr model. The amplitudes of the (ℓ, m) modes have different orders of magnitude, because of the missing factor M/D_L when dropping the Kerr assumption. Hence, the prior in log-amplitude of the fundamental mode is now $\log_{10}(A_{22}) \in [-25, -17)$. The priors in the remaining parameters are the same as in the previous section. Finally, we apply an additional set of constraints on the subdominant frequency and damping time to be within $\pm 25\%$ of the GR expectation.

Using the fitting formulae in [41], we can compare the mass and spin measurement obtained from the $(2,2)$ parameters and from the subdominant (ℓ, m) parameters. Furthermore, based on the measurement of the $(2,2)$ mode, we can infer the measured deviation on the frequency of the subdominant (ℓ, m) mode, $\delta f_{\ell m}$. Table II lists the rates of BBH ringdown signals per year that constrain GR within $\delta f_{\ell m} \pm 20\%$ at the 90% credible level. The results are summarized in Fig. 2.

Network	$\delta f_{\ell m} \leq \pm 20\%$
Adv. LIGO	$0.026^{+0.028}_{-0.014}$
A+	$0.27^{+0.30}_{-0.15}$
Voyager	$1.34^{+1.47}_{-0.73}$

TABLE II. Rates of BBH ringdown signals per year (yr^{-1}) with strong support for the presence of a second mode ($\mathcal{B}_{AB} > 3.2$) where deviations of the GR frequencies are constrained to within $\delta f_{\ell m} \leq \pm 20\%$ at the 90% credible level. We only show the rates for the population with uniform mass-ratio distribution ($\beta_q = 0$), since we know from the previous section that rates for a population with $\beta_q = 6.7$ will be lower.

V. CONCLUSIONS

In this paper we have applied for the first time the full Bayesian inference framework to a population of BH ringdowns derived from the observational population models published by the LIGO Scientific and Virgo Collaborations. Furthermore, we have allowed for completely variable ringdown phases, inclination angles, polarization angles and sky locations, contrary to previous works that have fixed one or more of these parameters for simplicity [13, 46, 47].

Within the Bayesian model selection framework, future generations of LIGO detectors will likely deliver measur-

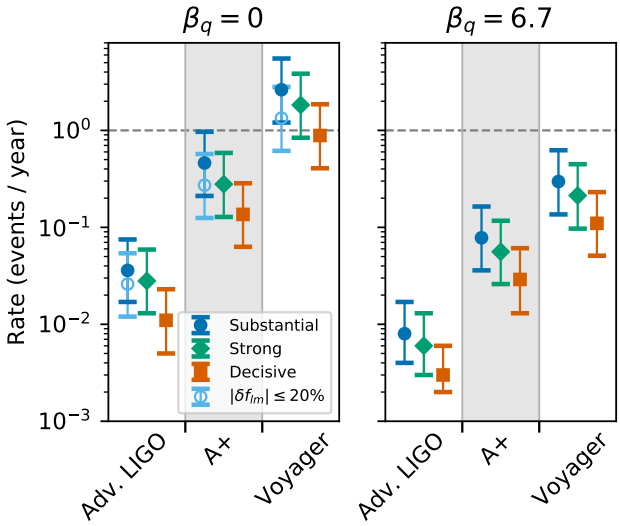

FIG. 2. Expected rates of BBH mergers for which two ringdown modes can be observed and resolved. We consider two population models corresponding to $\beta_q = \{0, 6.7\}$. Shown are the rate of events that have "substantial", "strong", and "decisive" Bayesian evidence (using the nomenclature of Ref. [32]) for a two-mode Kerr hypothesis relative to a single-mode hypothesis (filled circles, diamonds, and squares, respectively). Of the events that have substantial evidence, we perform a followup analysis in which the frequency and damping time of the subdominant mode is allowed to deviate from the expected GR value. The rate of events for which the deviation from GR of the subdominant frequency $|\delta f_{lm}|$ is constrained to be $\leq 20\%$ is given by the open circles.

able subdominant QNM modes from BBH mergers over the next decade. However, resolvability of the subdominant frequencies is technically challenging, and accurate tests of the no-hair theorem might only be possible in very few cases. These results are in agreement with previously published works [14, 15], where the ringdown SNR was used to determine the measurability and resolvability of QNMs.

Merger population models from gravitational-wave observations are still largely uncertain. The third observing run of Advanced LIGO and Virgo might be uncovering a new population of NSBH and other previously unobserved types of mergers, which could boost the rates of measurable and resolvable subdominant modes. Hence, the rates obtained in this work might turn out to be pessimistic as more gravitational-wave detections are made available.

VI. ACKNOWLEDGMENTS

We are thankful to Swetha Bhagwat, Duncan Brown, Evan Goetz, Scott Hughes, Alexander H. Nitz, Paolo Pani and Frans Pretorius for useful comments and discussions. We are especially grateful to Ssohrab Borhanian and Bangalore Sathyaprakash for providing us with the fits for the ringdown mode amplitudes in [8]. MC acknowledges support from NSF grant PHY-1607449, the Simons Foundation, and the Canadian Institute For Advanced Research (CIFAR). Computations have been performed on the Atlas cluster of the Albert Einstein Institute (Hannover).

[1] C. V. Vishveshwara, "Scattering of Gravitational Radiation by a Schwarzschild Black-hole," *Nature*, vol. 227, pp. 936–938, 1970.

[2] S. Chandrasekhar and S. L. Detweiler, "The quasi-normal modes of the Schwarzschild black hole," *Proc. Roy. Soc. Lond.*, vol. A344, pp. 441–452, 1975.

[3] K. D. Kokkotas and B. G. Schmidt, "Quasinormal modes of stars and black holes," *Living Rev. Rel.*, vol. 2, p. 2, 1999.

[4] E. Berti, V. Cardoso, and A. O. Starinets, "Quasinormal modes of black holes and black branes," *Classical and Quantum Gravity*, vol. 26, no. 16, p. 163001, 2009.

[5] O. Dreyer, B. J. Kelly, B. Krishnan, L. S. Finn, D. Garrison, and R. Lopez-Aleman, "Black hole spectroscopy: Testing general relativity through gravitational wave observations," *Class. Quant. Grav.*, vol. 21, pp. 787–804, 2004.

[6] E. Berti, V. Cardoso, and C. M. Will, "Gravitational-wave spectroscopy of massive black holes with the space interferometer lisa," *Phys. Rev. D*, vol. 73, p. 064030, Mar 2006.

[7] I. Kamaretsos, M. Hannam, S. Husa, and B. S. Sathyaprakash, "Black-hole hair loss: Learning about binary progenitors from ringdown signals," *Phys. Rev. D*, vol. 85, p. 024018, Jan 2012.

[8] S. Borhanian, K. G. Arun, H. P. Pfeiffer, and B. S. Sathyaprakash, "Signature of horizon dynamics in binary black hole gravitational waveforms," 2019.

[9] S. A. Hughes, A. Apte, G. Khanna, and H. Lim, "Learning about black hole binaries from their ringdown spectra," *Phys. Rev. Lett.*, vol. 123, no. 16, p. 161101, 2019.

[10] A. Apte and S. A. Hughes, "Exciting black hole modes via misaligned coalescences: I. Inspiral, transition, and plunge trajectories using a generalized Ori-Thorne procedure," *Phys. Rev.*, vol. D100, no. 8, p. 084031, 2019.

[11] H. Lim, G. Khanna, A. Apte, and S. A. Hughes, "Exciting black hole modes via misaligned coalescences: II. The mode content of late-time coalescence waveforms," *Phys. Rev.*, vol. D100, no. 8, p. 084032, 2019.

[12] E. E. Flanagan and S. A. Hughes, "Measuring gravitational waves from binary black hole coalescences: 1. Signal-to-noise for inspiral, merger, and ringdown," *Phys. Rev.*, vol. D57, pp. 4535–4565, 1998.

[13] E. Berti, J. Cardoso, V. Cardoso, and M. Cavaglià, "Matched-filtering and parameter estimation of ringdown waveforms," *Phys. Rev. D*, vol. 76, p. 104044, Nov 2007.

[14] E. Berti, A. Sesana, E. Barausse, V. Cardoso, and K. Belczynski, "Spectroscopy of Kerr black holes with Earth- and space-based interferometers," *Phys. Rev. Lett.*, vol. 117, no. 10, p. 101102, 2016.

[15] V. Baibhav and E. Berti, "Multimode black hole spectroscopy," *Phys. Rev.*, vol. D99, no. 2, p. 024005, 2019.

[16] B. P. Abbott *et al.*, "Binary Black Hole Population Properties Inferred from the First and Second Observing Runs of Advanced LIGO and Advanced Virgo," 2018.

[17] LIGO Scientific Collaboration and Virgo Collaboration, "GraceDB: S190814bv." https://gracedb.ligo.org/superevents/S190814bv/.

[18] LIGO Scientific Collaboration and Virgo Collaboration, "GraceDB: S190910d." https://gracedb.ligo.org/superevents/S190910d/.

[19] C. M. Biwer, C. D. Capano, S. De, M. Cabero, D. A. Brown, A. H. Nitz, and V. Raymond, "PyCBC inference: A python-based parameter estimation toolkit for compact binary coalescence signals," *Publications of the Astronomical Society of the Pacific*, vol. 131, p. 024503, jan 2019.

[20] A. Nitz *et al.*, "gwastro/pycbc." https://doi.org/10.5281/zenodo.3265452, July 2019.

[21] The LIGO Scientific Collaboration and the Virgo Collaboration, "GWTC-1: A Gravitational-Wave Transient Catalog of Compact Binary Mergers Observed by LIGO and Virgo during the First and Second Observing Runs," 2018.

[22] A. H. Nitz, T. Dent, G. S. Davies, S. Kumar, C. D. Capano, I. Harry, S. Mazzon, L. Nuttall, A. Lundgren, and M. Tpai, "2-OGC: Open Gravitational-wave Catalog of binary mergers from analysis of public Advanced LIGO and Virgo data," 2019.

[23] A. H. Nitz, C. Capano, A. B. Nielsen, S. Reyes, R. White, D. A. Brown, and B. Krishnan, "1-OGC: The first open gravitational-wave catalog of binary mergers from analysis of public Advanced LIGO data," *Astrophys. J.*, vol. 872, no. 2, p. 195, 2019.

[24] J. M. Antelis and C. Moreno, "An independent search of gravitational waves in the first observation run of advanced LIGO using cross-correlation," *Gen. Rel. Grav.*, vol. 51, no. 5, p. 61, 2019.

[25] B. Zackay, L. Dai, T. Venumadhav, J. Roulet, and M. Zaldarriaga, "Detecting Gravitational Waves With Disparate Detector Responses: Two New Binary Black Hole Mergers," 2019.

[26] T. Venumadhav, B. Zackay, J. Roulet, L. Dai, and M. Zaldarriaga, "New Binary Black Hole Mergers in the Second Observing Run of Advanced LIGO and Advanced Virgo," 2019.

[27] The LIGO Scientific Collaboration and the Virgo Collaboration, "Observation of gravitational waves from a binary black hole merger," *Phys. Rev. Lett.*, vol. 116, no. 6, p. 061102, 2016.

[28] The LIGO Scientific Collaboration and the Virgo Collaboration, "Tests of general relativity with GW150914," *Phys. Rev. Lett.*, vol. 116, no. 22, p. 221101, 2016. [Erratum: Phys. Rev. Lett.121,no.12,129902(2018)].

[29] G. Carullo, W. Del Pozzo, and J. Veitch, "Observational Black Hole Spectroscopy: A time-domain multimode analysis of GW150914," 2019.

[30] M. Giesler, M. Isi, M. Scheel, and S. Teukolsky, "Black hole ringdown: the importance of overtones," 2019.

[31] M. Isi, M. Giesler, W. M. Farr, M. A. Scheel, and S. A. Teukolsky, "Testing the no-hair theorem with GW150914," *Phys. Rev. Lett.*, vol. 123, no. 11, p. 111102, 2019.

[32] R. E. Kass and A. E. Raftery, "Bayes Factors," *J. Am. Statist. Assoc.*, vol. 90, no. 430, pp. 773–795, 1995.

[33] J. Annis, N. J. Evans, B. J. Miller, and T. J. Palmeri, "Thermodynamic integration and steppingstone sampling methods for estimating bayes factors: A tutorial," *Journal of mathematical psychology*, vol. 89, pp. 67–86, 2019.

[34] J. Veitch *et al.*, "cpnest." https://doi.org/10.5281/zenodo.835874, July 2017.

[35] K. S. Thorne, "300 years of gravitation," in *Gravitational radiation* (S. Hawking and W. Israel, eds.), Cambridge University Press, 1987.

[36] S. A. Teukolsky, "Rotating black holes - separable wave equations for gravitational and electromagnetic perturbations," *Phys. Rev. Lett.*, vol. 29, pp. 1114–1118, 1972.

[37] E. W. Leaver, "An Analytic representation for the quasi normal modes of Kerr black holes," *Proc. Roy. Soc. Lond.*, vol. A402, pp. 285–298, 1985.

[38] E. Berti, V. Cardoso, and M. Casals, "Eigenvalues and eigenfunctions of spin-weighted spheroidal harmonics in four and higher dimensions," *Phys. Rev.*, vol. D73, p. 024013, 2006. [Erratum: Phys. Rev.D73,109902(2006)].

[39] M. A. Cabero Müller, *Gravitational-wave astronomy with compact binary coalescences: from blip glitches to the black hole area increase law.* PhD thesis, Leibniz Universität Hannover, 2018.

[40] M. Cabero, C. D. Capano, O. Fischer-Birnholtz, B. Krishnan, A. B. Nielsen, A. H. Nitz, and C. M. Biwer, "Observational tests of the black hole area increase law," *Phys. Rev. D*, vol. 97, p. 124069, Jun 2018.

[41] E. Berti, V. Cardoso, and C. M. Will, "On gravitational-wave spectroscopy of massive black holes with the space interferometer LISA," *Phys. Rev.*, vol. D73, p. 064030, 2006.

[42] W. Tichy and P. Marronetti, "The Final mass and spin of black hole mergers," *Phys. Rev.*, vol. D78, p. 081501, 2008.

[43] F. Hofmann, E. Barausse, and L. Rezzolla, "The final spin from binary black holes in quasi-circular orbits," *Astrophys. J.*, vol. 825, no. 2, p. L19, 2016.

[44] LIGO Scientific Collaboration, "LIGO Algorithm Library - LALSuite." https://github.com/lscsoft/lalsuite.

[45] P. A. R. Ade *et al.*, "Planck 2015 results. XIII. Cosmological parameters," *Astron. Astrophys.*, vol. 594, p. A13, 2016.

[46] S. Bhagwat, M. Cabero, C. D. Capano, B. Krishnan, and D. A. Brown, "Detectability of the subdominant mode in a binary black hole ringdown," 2019.

[47] S. Gossan, J. Veitch, and B. S. Sathyaprakash, "Bayesian model selection for testing the no-hair theorem with black hole ringdowns," *Phys. Rev.*, vol. D85, p. 124056, 2012.

[48] The LIGO Scientific Collaboration, "Unofficial sensitivity curves (asd) for aligo, kagra, virgo, voyager, cosmic explorer and et." https://dcc.ligo.org/LIGO-T1500293/public, 2019.

[49] B. Sathyaprakash *et al.*, "Scientific Objectives of Einstein Telescope," *Class. Quant. Grav.*, vol. 29, p. 124013, 2012. [Erratum: Class. Quant. Grav.30,079501(2013)].

[50] B. Sathyaprakash *et al.*, "Scientific Potential of Einstein Telescope," in *Proceedings, 46th Rencontres de Moriond on Gravitational Waves and Experimental Gravity: La Thuile, Italy, March 20-27, 2011*, pp. 127–136, 2011.

[51] M. Punturo *et al.*, "The Einstein Telescope: A third-generation gravitational wave observatory," *Class. Quant. Grav.*, vol. 27, p. 194002, 2010.

[52] D. Reitze *et al.*, "Cosmic Explorer: The U.S. Contribution to Gravitational-Wave Astronomy beyond LIGO," 2019.

[53] K. Danzmann and A. Rudiger, "LISA technology - Concept, status, prospects," *Class. Quant. Grav.*, vol. 20, pp. S1–S9, 2003.

[54] S. Bhagwat, M. Okounkova, S. W. Ballmer, D. A. Brown, M. Giesler, M. A. Scheel, and S. A. Teukolsky, "On choosing the start time of binary black hole ringdowns," *Physical Review D*, vol. 97, no. 10, p. 104065, 2018.

[55] E. Berti, K. Yagi, H. Yang, and N. Yunes, "Extreme Gravity Tests with Gravitational Waves from Compact Binary Coalescences: (II) Ringdown," *Gen. Rel. Grav.*, vol. 50, no. 5, p. 49, 2018.

[56] V. Cardoso and P. Pani, "Testing the nature of dark compact objects: a status report," *Living Rev. Rel.*, vol. 22, no. 1, p. 4, 2019.

[57] A. Maselli, P. Pani, L. Gualtieri, and E. Berti, "Parametrized ringdown spin expansion coefficients: a data-analysis framework for black-hole spectroscopy with multiple events," 2019.

[58] F. Moulin, A. Barrau, and K. Martineau, "An overview of quasinormal modes in modified and extended gravity," *Universe*, vol. 5, no. 9, p. 202, 2019.